V_{OH-Be}—a new and unusual member in the family of V centres

2002 J. Phys.: Condens. Matter 14 8881

(http://iopscience.iop.org/0953-8984/14/38/311)

INSTITUTE OF PHYSICS PUBLISHING JOURNAL OF PHYSICS: CONDENSED MATTER

J. Phys.: Condens. Matter **14** (2002) 8881–8888 PII: S0953-8984(02)36970-4

V_{OH-Be}—a new and unusual member in the family of V centres

S A Dolgov[1], V Isakhanyan[2], T Kärner[1,3], A Maaroos[1] and S Nakonechnyi[2]

[1] Institute of Physics, University of Tartu, Riia 142, 51014 Tartu, Estonia
[2] University of Tartu, Ülikooli 18, 51014 Tartu, Estonia

E-mail: tiit@fi.tartu.ee

Received 14 May 2002, in final form 29 August 2002
Published 12 September 2002
Online at stacks.iop.org/JPhysCM/14/8881

Abstract

In Be-doped MgO crystals a new V centre has been discovered whose physical properties differ significantly from those of other V centres. The centre can be observed by means of EPR at room temperature; the shift of its g-factor from the free electron value is about 1.6 times smaller than that of a V_{OH} centre, the optical absorption band is shifted by $\sim$1 eV to higher energies, and the thermal destruction of the centre through the loss of a hole takes place at about 400 K. The axial symmetry of the centre and the hyperfine structure of its EPR spectrum suggest the following model of the centre: Be^{2+}–O^-–v_c–OH^-. The specific physical properties of the V_{OH-Be} centre are explained by an interaction of the effective electric dipole, created by the off-centre position of the Be^{2+} ion substituting for the Mg^{2+}, with the nearby localized hole.

1. Introduction

In alkaline-earth oxides, the centres, generated by trapping of holes by cation vacancies, are referred to as V^- centres. The excess negative charge of the centres can be compensated by another trapped hole (V^0 centre) or various aliovalent impurities at the neighbouring anion sites (V_{OH}, V_F centres) or cation sites (V_{Al} centres). An overview of the properties of V centres can be found in [1, 2].

The V centres can be created by ionizing radiation. The thermal stability of the centres depends on the presence and type of the charge-compensating impurity. The position of the thermoluminescence (TL) peaks related to the thermal release of the holes from these V centres varies from 335 K (V_{OH} centres) to 420 K (V^- centres, for heating rate 10 K min^{-1}) [3]. The optical absorption bands related to the V centres lie at 2.2–2.3 eV [1]. The V centres are EPR active. The EPR signal can be observed at low temperatures ($T \lesssim 80$ K); at higher

[3] Author to whom any correspondence should be addressed.

temperatures the width of the EPR lines begins to grow and their amplitude declines. The perpendicular component of the g-factor of the axially symmetric V centres lies in the range of 2.0385 (V^- centre) to 2.0408 (V^0 centre) [1, 4].

We report the discovery of a new V centre in Be-doped MgO whose physical properties differ significantly from those of other V centres in MgO.

2. Experimental details

The MgO:Be single crystals were grown at the Institute of Physics, University of Tartu, by a variation of the arc fusion technique [5] using an arc furnace with two carefully cleaned spectrographic-grade graphite electrodes. The starting material was a mixture of high-purity MgO and BeO. The mixture was stirred, heated 1 h at ∼1520 K to remove moisture and chemisorbed water and decompose any unwanted Be compounds, and compressed. Taking into account that at the temperature of crystal growth (∼3075 K), a rapid evaporation of BeO was expected, the concentration of BeO in the starting powder was taken as 2000 ppm—that is, twice as high as the greatest substitutional solubility of Be ions in MgO given in the literature [6, 7]. As a result, crystals up to 15 × 15× 10 mm^3 were formed. The average content of the most common transition metal impurities in these crystals was about 10 ppm. In MgO, Be^{2+} substitutes for Mg^{2+} and was found to be present both in the form of isolated ions and within defect complexes. In the first case, under irradiation it was able to trap both electrons and holes, forming Be^{1+} and Be^{2+} O^- centres, respectively. The estimated content of Be in the MgO:Be crystals was about 100 ppm.

The EPR and TL of the MgO:Be single crystals have been measured. The EPR spectra were measured with an X-band (9.928 GHz) ERS 231 spectrometer. A continuous-flow helium cryostat (Oxford Instruments, ESR900) was used to keep the samples at the necessary temperature. Pulse annealing of the samples was carried out to determine the thermal stability of the observed EPR-active centre. On pulse annealing the crystals were kept, after a fast heating up, at the required temperature for 2 min and then cooled down to the measurement temperature. The measured EPR spectra were analysed using the computer program EPR-NMR (Department of Chemistry, University of Saskatchewan, Canada, 1993). The optical absorption was measured using a Jasco V-550 spectrophotometer.

3. Experimental results

When MgO:Be crystals are subjected to x-irradiation, a new paramagnetic centre is formed. The centre is stable at room temperature (RT). The paramagnetic resonance spectrum of this centre can be observed in the temperature range of 40 K to RT. The EPR spectrum of the centre measured at RT with the orientation of the magnetic field $\boldsymbol{B}$ parallel to a ⟨100⟩ crystal axis is shown in figure 1. Below 40 K the saturation of the EPR signal of the centre prevents its detection. We noted no changes in the EPR spectra measured at various temperatures. However, we observed another EPR signal in the MgO:Be crystals x-irradiated at 77 K. The symmetry of this EPR spectrum changes from orthorhombic for $T < 30$ K to axial for $T > 60$ K. We assigned this spectrum to a hole trapped near a substitutional Be^{2+} ion (Be^{2+} O^- centre). The observed change in its EPR spectrum we related to a motional averaging of the spectrum due to a noncentral position of the small Be^{2+} ion in a cation site. These results will be reported elsewhere.

The angular dependence of the EPR spectrum, as well as the EPR spectra measured for certain particular orientations of the crystal in the magnetic field, are shown in figure 2. The

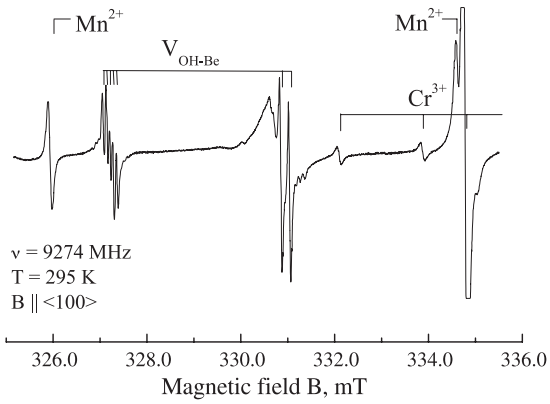

Figure 1. The RT EPR spectrum of V_{OH-Be} centres: a high-field doublet $g_{\|} = 2.0023$) and a low-field quintet ($g_{\perp} = 2.0250$), generated by a superposition of two pairs (corresponding to $m_H = \pm 1/2$) of shf quartets ($m_{Be} = \pm 1/2, \pm 3/2$). The broad line at $B \simeq 330.8$ mT belongs to the V_{OH} centres with their axes parallel to the external magnetic field $\boldsymbol{B}$.

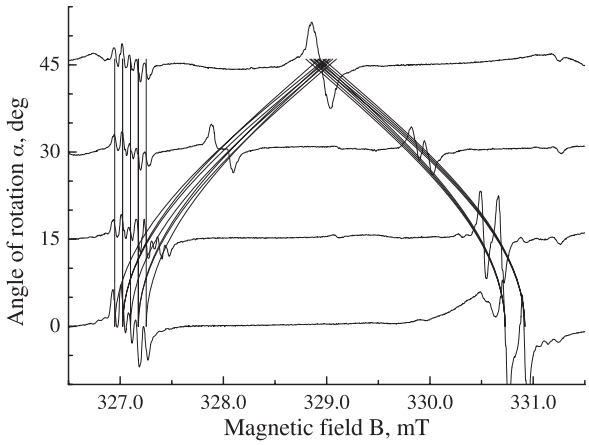

Figure 2. The calculated angular dependence of the EPR spectrum and measured EPR spectra of the V_{OH-Be} centres. The magnetic field lies in the {001} plane; α is the angle between the magnetic field direction and a ⟨100⟩ crystal axis. Experimental spectra are given for $\alpha = 0$, 15, 30, 45°.

magnetic field lies in a {001} plane; α is the angle between the magnetic field direction and a ⟨100⟩-type crystal axis. The angular dependence depicted is the calculated one. At most crystal orientations, the spectral lines are not resolved and their positions cannot be exactly measured.

The spectrum consists of three groups of lines for general orientation of the magnetic field $\boldsymbol{B}$, consistent with ⟨100⟩-type axial symmetry of the centre. Each group, in its turn, contains two four-line groups. The relative positions of the lines in these eight-line groups depend on the orientation of the crystal in the external magnetic field. For that reason, when a magnetic field is directed along the high-symmetry axes of the centre (and the crystal), the positions of several lines coincide and the number of observable lines will be reduced. Hence, for the magnetic field directed along the defect axis (the ⟨100⟩ crystal axis), the number of lines is reduced to two; for the magnetic field directed perpendicularly to the defect axis, we

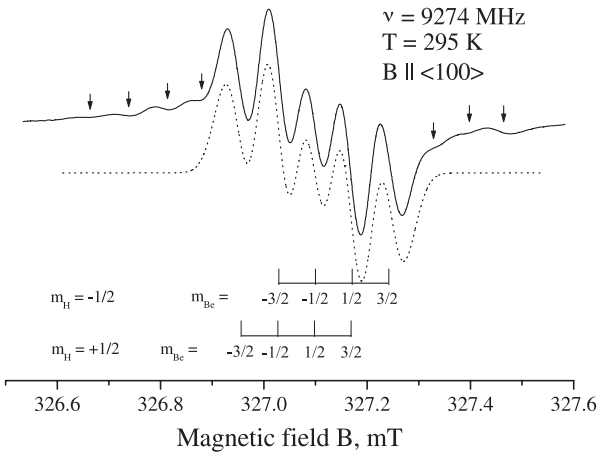

Figure 3. The low-field part of the EPR spectrum of V_{OH-Be} centres: measured (solid curve) and simulated (dotted curve) spectra. The calculated positions of the individual EPR lines and the corresponding spin projection quantum numbers (in the high-field approximation) are indicated. The weak spectral lines presumably relating to V_{OH-Be} centres with rhombic symmetry (see the text) are marked with arrows.

observe a group of five lines (figure 3). Such behaviour suggests a hyperfine interaction with two magnetic ions with nuclear spins $1/2$ and $3/2$, and specific values of the corresponding superhyperfine (shf) constants. Namely: for the magnetic field orientation perpendicular to the defect axis, the two constants must be approximately equal; for the magnetic field parallel to the defect axis, the hyperfine constant associated with the nuclear spin $3/2$ must be close to zero. In figure 3, the calculated positions of the individual EPR lines are shown and the spin projection quantum numbers (in the high-field approximation) are given.

Another interesting feature in figure 3 is a set of weak spectral lines around the five main lines, marked with arrows. These lines were invariably present for all the measured crystals but they were too weak for us to follow their angular dependence.

The thermal stability of the centres was measured using both the pulse annealing and TL methods and was, at a heating rate $1/6$ K s^{-1}, approximately 400 K. In optical absorption the presence of the new centres manifests itself in an additional broad absorption band extending from 2.5 to 4.0 eV (figure 4).

4. Discussion

4.1. Spin Hamiltonian parameters and the model of the centre

The nucleus with $I = 3/2$ is obviously the doped ^{9}Be; the most likely candidate for being the $I = 1/2$ nucleus is ^{1}H, because:

(1) the MgO:Be crystals grown were cloudy, which is characteristic of MgO crystals with a high content of hydrogen [8];
(2) in the low-temperature EPR spectra of the as-grown MgO:Be single crystals, x-irradiated at liquid nitrogen temperature or RT, we observed a strong characteristic doublet EPR spectrum of V_{OH} centres [9];
(3) the magnitude of the hyperfine doublet splitting at $\boldsymbol{B} \parallel \langle 100 \rangle$ of the new centre is very close to that of a V_{OH} centre.

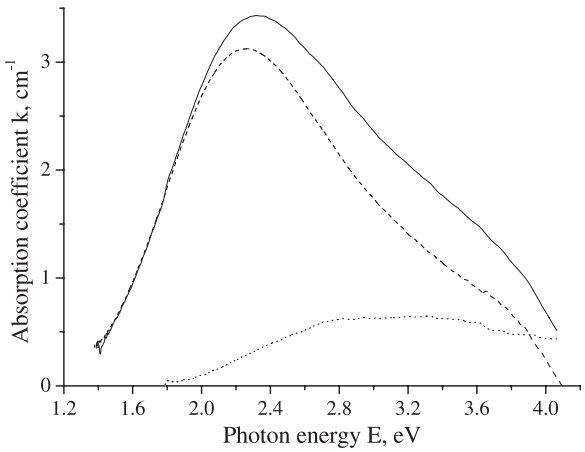

Figure 4. The additional optical absorption of MgO:Be (solid curve) and MgO:OH crystals (dashed curve) induced by x-irradiation (295 K, 50 kV, 100 Gy), measured at RT. The dotted curve depicts the difference of these two absorption curves. The absorption spectra were normalized with respect to the low-energy side of the absorption peak of the V_{OH} centres at 2.3 eV.

Therefore, we attribute the observed spectrum to a linear defect which we refer to as a V_{OH-Be} centre: Be^{2+}–O^-–v_c–OH^-.

The EPR spectrum and its angular dependence can be described using the following spin Hamiltonian:

$$H = \beta \boldsymbol{S}\mathbf{g}\boldsymbol{B} + h\boldsymbol{S}\mathbf{A}_{\mathrm{H}}\boldsymbol{I}_{\mathrm{H}} + h\boldsymbol{S}\mathbf{A}_{\mathrm{Be}}\boldsymbol{I}_{\mathrm{Be}} - g_{\mathrm{H}}\beta_{\mathrm{N}}\boldsymbol{B}\cdot\boldsymbol{I}_{\mathrm{H}} - g_{\mathrm{Be}}\beta_{\mathrm{N}}\boldsymbol{B}\cdot\boldsymbol{I}_{\mathrm{Be}} + h\boldsymbol{I}_{\mathrm{Be}}\mathbf{P}\boldsymbol{I}_{\mathrm{Be}},$$

where the first term describes the electron Zeeman interaction, the second and the third terms the shf interaction, the following two terms the nuclear Zeeman interaction, and the last term the nuclear quadrupole interaction due to the Be nucleus with the nuclear spin $I_{\mathrm{Be}} = 3/2$.

The quadrupole term was included in the hope that it may explain the shape of the low-field five-line group and the nature of the weak spectral lines around this group (figure 2). However, a detailed investigation showed that this was not the case; the observed EPR spectrum could be simulated without any quadrupole contribution (see dotted curve of figure 2) and the weak spectral lines in figure 2, marked with arrows, are not related to forbidden $\Delta M = 2$ transitions made partly allowed by quadrupole interaction. All our attempts to simulate both the central part of the spectrum and these weaker side lines as forbidden lines failed regardless of the size of the nuclear quadrupole factor P and the symmetry of the nuclear quadrupole parameter matrix $\mathbf{P}$. Apparently the quadrupole term is too small to be detected by means of EPR. This agrees with a crude numerical estimation of the size of the quadrupole interaction. Taking into account the $1s^2$ electron configuration of a Be^{2+}, which makes it possible to neglect in quadrupole interaction calculations the unpaired spin density moving in p orbitals and the Sternheimer anti-shielding factor [10, 11], the nuclear quadrupole factor in this simple point charge approximation is

$$P = \frac{e^2 Q}{4I_{\mathrm{Be}}(2I_{\mathrm{Be}} - 1)}\frac{2}{R^3} \approx 0.02\ \mathrm{MHz},$$

where e is the elementary charge, the electric quadrupole moment of the Be nucleus $Q = 0.053 \times 10^{-24}$ cm^2 [10], and $R = 0.24$ nm is the nearest-neighbour distance in MgO. Our measurements show that because of the small ionic radius of Be^{2+} (0.034 nm versus 0.074 for Mg^{2+} [12]), the Be ions retain a certain mobility even at RT and tend to form associations

Table 1. A comparison of physical properties of V centres in MgO.

Centre	$\Delta g = g_\perp - g_e$	Temperature of thermal destruction (K)	Position of optical absorption band (eV)
V_{OH-Be}	0.0227	400	3.0–3.5
V_{OH}	0.0373 [1]	335 [3]	2.21[14]
V_{Al}	0.0362 [1]	370 [3]	2.3
V^0	0.0385 [4]	345 [3]	2.36 [4]
V^-	0.0362 [1]	420 [3]	2.33 [1]

with various defects. It seems possible that the observed weak spectral lines relate to rhombic V_{OH-Be} centres with Be^{2+} in a non-axial position.

Assuming an axial symmetry of the centre, a least-squares fitting of the calculated spectrum to the experimental data gave the following parameters for the spin Hamiltonian: $g_\perp = 2.025 \pm 0.0002$, $g_\parallel = 2.0023 \pm 0.0002$, $A_{H_\perp} = \pm(2.085 \pm 0.025)$ MHz, $A_{H_\parallel} = \pm(5.212 \pm 0.025)$ MHz, $A_{Be_\perp} = \pm(2.01 \pm 0.06)$ MHz, $A_{Be_\parallel} = \pm(0.00 \pm 0.06)$ MHz. The main components of the shf tensor related to H^+ are very close to those of a V_{OH} centre. The isotropic shf constant $a_H = (A_{H_\parallel} + 2A_{H_\perp})/3 \approx 0.353$ MHz is characteristic of a neighbouring nucleus beyond the second shell and allows us to approximate the anisotropic shf interaction by a point dipole–dipole interaction. In this case, the anisotropic shf constant $b_H = (A_{H_\parallel} - A_{H_\perp})/3 = 95.625\, g_H/r^3$ MHz [10], where g_H is the nuclear g-factor and r is the distance between the nucleus and the defect centre in atomic units. The analysis of these constants is basically the same as in [9]; therefore, we concentrate on the shf interaction related to the Be nucleus.

The values of the isotropic and anisotropic shf constants are as follows: $a_{Be} = 1.34$ MHz, $b_{Be} = 0.67$ MHz. Comparing a_{Be} to the isotropic hyperfine interaction constant for the unit spin density in the Be 2s orbital (451.6 MHz [13]) shows that the admixture of this orbital into the defect wavefunction is still very low. This is consistent with the tight binding of the hole localized near a cation vacancy. On this basis, and taking into account the above-mentioned $1s^2$ electron configuration of Be^{2+}, it still seems justified to consider the anisotropic shf interaction as a distant point dipole–dipole interaction. Using the calculated b_{Be} and taking $|g_{Be}| = 0.785$ [10], we obtain $r = 0.255$ nm $= 1.2\, a_0/2$, where a_0 is a lattice constant of MgO. Considering a possible relaxation of the Be^{2+} ion, this seems to be quite a reasonable result and shows that a Be^{2+} ion substitutes for a Mg^{2+} in a position that is a nearest neighbour of the localized hole. Consequently, the shf data seem to support the model of the centre given above.

4.2. Physical properties of the V_{OH-Be} centre

Many physical properties of the V_{OH-Be} centre—its g-factor, its thermal stability, its spin–lattice relaxation time, the position of its optical absorption peak—are substantially different from those of all other V-type centres in MgO. For example, because of the relatively short time taken for spin–lattice relaxation, the EPR spectra of V centres in MgO are barely visible at RT, whereas the EPR spectra of the V_{OH-Be} centre can be best recorded just at RT. Table 1 illustrates this difference further.

The model of the V_{OH-Be} centre with Be^{2+} relaxed away from the cation vacancy and the hole explains the relatively high thermal stability of the centre. Its thermal destruction through the loss of the hole takes place at about 400 K (heating rate: 10 K min^{-1}) while a V_{OH} and uncompensated V^- centre decay at 335 and 420 K, correspondingly [3]. Apparently,

the Be^{2+} ion in the noncentral position in a Mg^{2+} site acts as an electric dipole, stabilizing the hole. The increased depth of the ground-state level of a V_{OH-Be} centre manifests itself also in the absorption spectra of the MgO:Be crystal (figure 4) and in the diminished g-factor shift $\Delta g = g_\perp - g_e \simeq 2|\lambda|/\delta$, where g_e is the free electron g-factor, λ is the spin–orbit coupling parameter, and δ is the separation between the two lowest orbital energy levels. Figure 4 shows the x-irradiation-induced change in the absorption of a Be-doped MgO crystal and of a MgO crystal, grown from a water-soaked starting powder, and containing a large number ($\sim 10^{18}$ cm^{-3}) of V_{OH} centres. We refer later to the latter crystal as MgO:OH. A comparison of these curves shows that x-irradiation of MgO:Be crystals, as compared to MgO:OH crystals, creates an additional optical absorption in the region of 3–4 eV. It is known [15, 16] that the optical transitions observed in the absorption spectra are related to a small-polaron transition from one oxygen to the other oxygen neighbours of the cation vacancy (interpolaron transition); the g-factor shift, however, is related to the intrapolaron transition, whose energies in the case of V^- or V_{OH} centres equal $\sim$2.3 and $\sim$1.5 eV, respectively. For a V_{OH} centre, $\Delta g = 0.0373$; for a V_{OH-Be} centre, $\Delta g = 0.0227$; for the intrapolaron transition in the V_{OH-Be} centre, this gives $\delta \approx 2.5$ eV. If we assume that the ratios of the energies of interpolaron and intrapolaron transitions for the V_{OH} and V_{OH-Be} centres are the same, we get, for the energy of the intrapolaron transition in a V_{OH-Be} centre, 3.8 eV, which agrees reasonably well with the results of the optical absorption measurements (figure 4).

Finally, the low rate of the spin–lattice relaxation of a V_{OH-Be} centre, which makes it possible to observe the centre at RT, unlike the case for other V centres whose EPR lines have already begun to broaden at $T = 80$ K, can be explained on the grounds of the usual Kronig–Van Vleck mechanism of relaxation [17]. To see the effect of phonon-induced crystal-field modulations on the spin states, higher excited states of a non-zero orbital momentum must be mixed into the ground state with spin–orbit interaction. An increase in the separation of ground and excited energy levels leads to a weakening of the influence of spin–orbit interaction and manifests itself both in the change of the g-factor value and in the growth of the spin–lattice relaxation time.

5. Conclusions

In Be-doped MgO crystals a new V-type centre—the linear defect Be^{2+}–O^-–v_c–OH^- (the V_{OH-Be} centre)—is formed. The physical properties of this centre: its g-factor, its thermal stability, the position of the optical absorption, and the spin–orbit relaxation time, differ significantly from those of other V centres. The specific physical properties of the V_{OH-Be} centre derive from the fact that Be^{2+} ion, with an ionic radius considerably smaller than that of Mg^{2+}, relaxes away from the hole localized on an oxygen ion, lowering the energy of the ground state of the centre and increasing its separation from the excited states. This leads to a weakening of the influence of spin–orbit interaction and manifests itself both in the change of the g-factor value and in the growth of the spin–lattice relaxation time.

Acknowledgment

This work was supported by the Estonian Science Foundation (grant No 5027).

References

[1] Henderson B and Wertz J E 1979 *Defects in the Alkaline Earth Oxides* (London: Taylor&Francis)
[2] Chen Y and Abraham M M 1990 *J. Phys. Chem. Solids* **51** 747

[3] Kärner T, Malysheva A F, Maaroos A and Mürk V V 1980 *Sov. Phys.–Solid State* **22** 1178
[4] Kappers L A, Dravnieks F and Wertz J E 1974 *J. Phys. C: Solid State Phys.* **7** 1387
[5] Maaroos A 1982 *Trudy IF Akad. Nauk Est. SSR* **53** 49 (in Russian)
[6] Lacis I E and Valbis J A 1979 *Phys. Status Solidi* b **95** K21
[7] Mackrodt W C and Stewart R F 1979 *J. Phys. C: Solid State Phys.* **12** 5015
[8] Briggs A 1975 *J. Mater. Sci.* **10** 729
[9] Kirklin P W, Auzins P and Wertz J E 1965 *J. Phys. Chem. Solids* **26** 1067
[10] Spaeth J M, Niklas J R and Bartram R H 1992 *Structural Analysis of Point Defects in Solids (Springer Series in Solid-State Sciences)* (New York: Springer)
[11] Foley H M, Sternheimer R M and Tycko D 1954 *Phys. Rev.* **93** 734
[12] Shannon R D 1976 *Acta Crystallogr.* A **3** 759
[13] Morton J R and Preston K F 1978 *J. Magn. Reson.* **30** 577
[14] Kappers L A, Dravnieks F and Wertz J E 1972 *Solid State Commun.* **10** 1265
[15] Schirmer O F 1976 *Z. Phys.* B **24** 235
[16] Norgett M J, Stoneham A M and Pathak A P 1977 *J. Phys. C: Solid State Phys.* **10** 555
[17] Abragam A and Bleaney B 1970 *Electron Paramagnetic Resonance of Transition Ions* (Oxford: Clarendon)